

Novel artificial optical annular structures in the high latitude ionosphere over EISCAT

M. J. Kosch,¹ M. T. Rietveld,² A. Senior,¹ I. W. McCrea,³ A. J. Kavanagh,⁴ B. Isham,⁵ and F. Honary¹

Received 12 February 2004; revised 14 May 2004; accepted 20 May 2004; published XX Month 2004.

[1] The EISCAT low-gain HF facility has been used repeatedly to produce artificially stimulated optical emissions in the F-layer ionosphere over northern Scandinavia. On 12 November 2001, the high-gain HF facility was used for the first time. The pump beam zenith angle was moved in 3° steps along the north-south meridian from 3°N to 15°S, with one pump cycle per position. Only when pumping in the 9°S position were annular optical structures produced quite unexpectedly. The annuli were approximately centred on the pump beam but outside the -3 dB locus. The optical signature appears to form a cylinder, which was magnetic field-aligned, rising above the pump wave reflection altitude. The annulus always collapsed into the well-known optical blobs after ~60 s, whilst descending many km in altitude. All other pump beam directions produced optical blobs only. The EISCAT UHF radar, which was scanning from 3° to 15°S zenith angle, shows that enhanced ion-line backscatter persisted throughout the pump on period and followed the morphology of the optical signature. These observations provide the first experimental evidence that Langmuir turbulence can accelerate electrons sufficiently to produce the optical emissions at high latitudes. Why the optical annulus forms, and for only one zenith angle, remains unexplained. **INDEX TERMS:** 0310 Atmospheric Composition and Structure: Airglow and aurora; 2403 Ionosphere: Active experiments; 2407 Ionosphere: Auroral ionosphere (2704); 2451 Ionosphere: Particle acceleration. **Citation:** Kosch, M. J., M. T. Rietveld, A. Senior, I. W. McCrea, A. J. Kavanagh, B. Isham, and F. Honary (2004), Novel artificial optical annular structures in the high latitude ionosphere over EISCAT, *Geophys. Res. Lett.*, *31*, LXXXXX, doi:10.1029/2004GL019713.

1. Introduction

[2] A major goal in studying the ionosphere is to understand the fundamental physics governing the interaction between plasma and electromagnetic waves. One of the many manifestations of wave-plasma coupling is the production of artificial optical emissions in the F-layer ionosphere by high power high-frequency (HF) radio waves transmitted from the ground. This observational fact has only been recently

established at high latitudes [Kosch *et al.*, 2000; Pedersen and Carlson, 2001] but has been known for decades at lower latitudes [e.g., Bernhardt *et al.*, 1991, and references therein]. The emissions are produced by electrons accelerated by plasma turbulence, which then collide with the thermospheric neutrals. The optical wavelengths emitted are identical to those for natural auroras, primarily O(¹D) 630 and O(¹S) 557.7 nm [e.g., Gustavsson *et al.*, 2002]. Taking the collisional excitation of the vibrational states of N₂ into account, the effective electron energy threshold for 630 nm is ~3.5 eV, and for 557.7 nm it is ~4.5 eV [Haslett and Megill, 1974; Bernhardt *et al.*, 1991].

[3] From low latitude studies, the mechanism for producing artificial optical emissions has been attributed to either Langmuir turbulence [Gurevich *et al.*, 1985] or the tail of a Maxwellian velocity distribution of HF pump-enhanced electron temperature. However, the latter mechanism has been shown to be unrealistic by modelling [Mishin *et al.*, 2000; Gustavsson *et al.*, 2001], optical observations [Gustavsson *et al.*, 2002], and radar measurements of electron temperature [Gustavsson *et al.*, 2001; Rietveld *et al.*, 2003]. A third possibility is upper-hybrid turbulence, which Kosch *et al.* [2002a] have demonstrated experimentally to be linked to the artificial optical emissions, at least for high latitudes. This mechanism is supported by recent theoretical developments [e.g., Istomin and Leyser, 2003]. The result is perhaps not surprising as the upper-hybrid resonance altitude is below that for Langmuir turbulence, typically by 3–8 km. HF pump electromagnetic waves are efficiently converted into upper-hybrid electrostatic waves, which have a symbiotic relationship to pump-enhanced magnetic field-aligned density irregularities called striations [e.g., Istomin and Leyser, 1997]. Kosch *et al.* [2002b] have reported the link between striations and artificial optical emissions.

[4] Pump wave conversion to Langmuir electrostatic waves is accompanied by the simultaneous production of ion-acoustic waves [Robinson, 1989, 1997] to which incoherent backscatter radars are sensitive. Observations of enhanced ion-line (ion-acoustic waves) and plasma-line (Langmuir waves) backscatter just below the pump wave reflection altitude show that Langmuir turbulence is important for the initial few seconds after a pump wave is switched on [e.g., Honary *et al.*, 1999] before the pump-enhanced striations fully establish themselves. In addition, Honary *et al.* [1999] have shown that Langmuir turbulence persists when pumping on an electron gyro-harmonic frequency because the growth of striations is suppressed [e.g., Ponomarenko *et al.*, 1999; Kosch *et al.*, 2002a]. Hence, the HF pump wave can reach the Langmuir matching height without being dissipated by mode conversion into upper-

¹Communication Systems, Lancaster University, Lancaster, UK.

²EISCAT Scientific Association, Ramfjordbotn, Norway.

³Rutherford-Appleton Laboratory, Didcot, UK.

⁴High Altitude Observatory, National Center for Atmospheric Research, Boulder, Colorado, USA.

⁵EISCAT Scientific Association, Longyearbyen, Norway.

99 hybrid waves. It is during the search for artificial optical
 100 emissions linked to Langmuir turbulence accelerated electrons
 101 that the unexpected observations, reported below,
 102 were made.

103 [5] The experiment used the EISCAT HF pump facility
 104 [Stubbe, 1996], the EISCAT UHF radar [Rishbeth and van
 105 Eyken, 1993], both located at Ramfjordmoen, Norway
 106 (69.59°N, 19.23°E), and the DASI low-light-level imager
 107 [Kosch et al., 1998], located 50 km away at Skibotn,
 108 Norway (69.35°N, 20.36°E). The HF pump can form two
 109 steerable beams, $\sim 15^\circ$ wide (4–8 MHz) and $\sim 7.5^\circ$ wide
 110 (5.4–8 MHz). The former low-gain and latter high-gain
 111 beams can achieve a maximum ~ 300 MW and ~ 1.2 GW of
 112 effective isotropic radiated power (ERP), respectively. Past
 113 artificial optical emission experiments at EISCAT have
 114 focussed exclusively on low-gain wide-beam pumping
 115 [e.g., Kosch et al., 2000, 2002a; Rietveld et al., 2003].
 116 Below, we report on the first high-gain narrow-beam optical
 117 experiment. In addition, to facilitate stimulating Langmuir
 118 waves, it was necessary to select a pump frequency close to
 119 a gyro-harmonic. The gyro-frequency is a function of
 120 magnetic field strength and so varies slowly with altitude
 121 [Kosch et al., 2002a]. The 4th gyro-harmonic at 5.423 MHz
 122 is at ~ 215 km altitude over EISCAT.

123 2. Observations and Results

124 [6] On 12 November 2001 the high-gain HF pump was
 125 operated at 550 MW ERP and 5.423 MHz between 15:09
 126 and 18:22 UT. Between 15:09 and 16:55 UT the HF beam
 127 pointing direction was 9° south of vertical, operating with a
 128 2 min. on, 2 min. off cycle, and the EISCAT UHF radar was
 129 scanning through 3, 6, 9, 12 and 15° south of vertical,
 130 dwelling 4 min. on each position. Between 16:57 and
 131 18:22 UT the HF beam was scanning through 3° north,
 132 vertical, and 3, 6, 9, 12 and 15° south with a 2 min. on,
 133 1 min. off cycle, and the UHF radar was pointing 9° south
 134 of vertical. The radar modulation was the tau2 alternating
 135 code with an unambiguous range resolution of 5.4 km and
 136 temporal resolution of 5 s. Optical observations were made
 137 from Skibotn into the local zenith using a 50° field-of-view
 138 and narrow-band interference filters at either 557.7 (16:24–
 139 18:09 UT) or 630 nm (all other times). The reflection height
 140 of the 5.423 MHz wave was in the range ~ 220 –235 km for
 141 15–17 UT, rising in altitude thereafter. During this interval
 142 the peak plasma frequency remained >8 MHz, hence the HF
 143 pump wave did not penetrate the ionosphere.

144 [7] Figure 1 shows a sequence of 630 nm images for
 145 16:17:00–16:18:50 UT, with 10 s integration. The unex-
 146 pected annular optical emission structure, which developed
 147 when the HF beam was pointing 9° south, is clearly seen.
 148 The HF reflection altitude was ~ 235 km. The slow develop-
 149 ment of the emission brightness is due to the long
 150 radiative lifetime of O^1D , which is ~ 30 s at 235 km altitude
 151 [Gustavsson et al., 2001]. Mapping the HF beam -3 dB
 152 locus in free space onto the image at 235 km altitude shows
 153 that the optical annulus is centred around the beam edge,
 154 where the gradient in HF field strength is greatest. After
 155 ~ 60 s, the emission region collapses into a blob located
 156 close to the magnetic field line direction. This phenomenon
 157 repeated itself over several cycles but it was never possible
 158 to produce a stable annulus. The end state blob is consistent

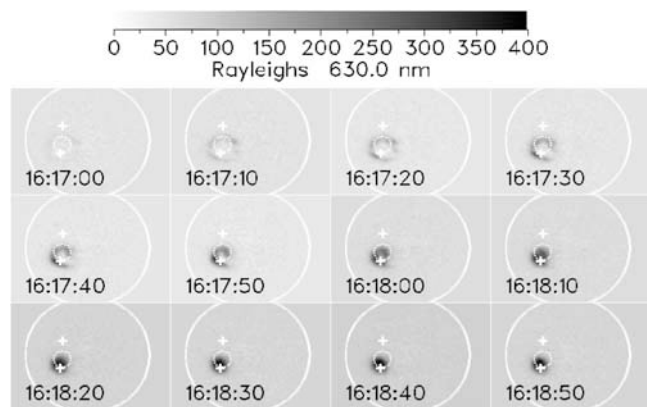


Figure 1. A sequence of images showing the development of the artificial optical structure on 12 November 2001. The images are calibrated into Rayleighs at 630 nm and have 10 s integration. North and east are to the top and right, respectively. Each image is taken in the zenith from Skibotn and has a 50° field of view (large circle). The HF pump turns on at 16:17:00 UT and off at 16:19:00 UT, after which the optical blob simply fades away. The -3 dB locus of the pump beam is shown as a small circle (beam width = 7.4°), projected at 235 km altitude and tilted 9° south of the HF facility at Ramfjordmoen assuming free space propagation. The upper cross shows the location of the HF transmitter whilst the lower cross shows the magnetic field line direction (12.8° S), both projected at 235 km.

with all previous observations [e.g., Kosch et al., 2000; 159
 Gustavsson et al., 2001; Rietveld et al., 2003]. The maxi- 160
 mum annulus and blob brightness above background is 161
 ~ 100 and ~ 300 Rayleighs (R), respectively. The latter is 162
 exceptional as previous observations are typically <150 R 163
 [Kosch et al., 2000; Rietveld et al., 2003]. Optical observa- 164
 tions at 557.7 nm showed the same morphology with 165
 similar emission intensities. Again, the maximum brightness 166
 is exceptional as previous observations are typically <50 R 167
 [Gustavsson et al., 2002; Pedersen et al., 2003]. When the 168
 HF beam was pointed 6 or 12° south, a small fraction of the 169
 annulus would sometimes develop. For all other positions, 170
 only optical blobs were generated if they were visible at all. 171
 Given the 7.4° beam width, the beam pointing for producing 172
 complete annuli is surprisingly sensitive and must be a 173
 characteristic of the mechanism. In addition, despite the HF 174
 power density being double within the annulus, there is no 175
 detectable optical emission. To date, no theory can explain 176
 the morphology of the phenomenon. Haslett and Megill 177
 [1974] have also reported ring-like structures in artificial 178
 optical emissions. However, these have a different morphol- 179
 ogy in that theirs is a steady state phenomenon and the 180
 optical intensity in the centre of the pumped region is not 181
 zero. We believe that our observations show a quite differ- 182
 ent phenomenon to that described by Haslett and Megill 183
 [1974]. 184

[8] Figure 2 shows a single image for 557.7 nm, taken at 185
 16:37:05 UT with 5 s integration, for the same experimental 186
 geometry as Figure 1. The HF reflection altitude was 187
 ~ 230 km. The relatively short O^1S radiative lifetime of 188
 ~ 0.7 s gives a better time resolution. Although the annulus 189
 is not complete on the HF pumping cycle shown, rayed 190

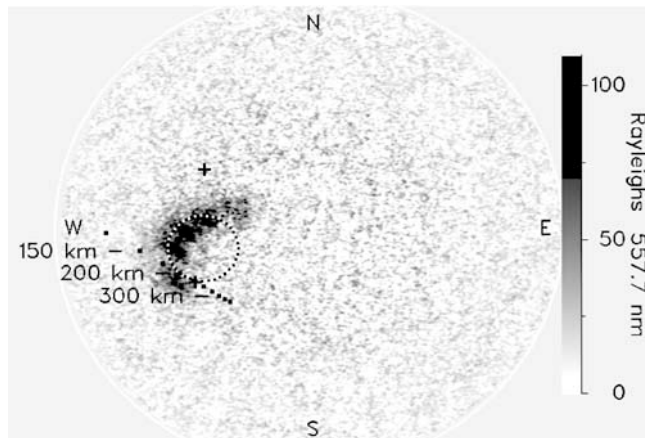


Figure 2. The artificial auroral structure at 16:37:05 UT on 12 November 2001, 5 s after HF pump turn on. The image has 5 s integration and is calibrated into Rayleighs at 557.7 nm. The image is taken in the zenith from Skibotn and has a 50° field of view (large circle). The -3 dB locus of the pump beam assuming free space propagation is shown as a small circle (beamwidth = 7.4°), projected at 230 km altitude and tilted 9° south of the HF facility at Ramfjordmoen. The upper cross shows the location of the HF transmitter whilst the lower cross shows the magnetic field line direction (12.8° S), both projected at 230 km. The dotted line represents the magnetic field line connected to Ramfjordmoen and the labels give altitude.

191 structures are clearly seen. These are not visible for 630 nm
 192 (Figure 1) because the long radiative lifetime of O^1D is
 193 roughly the same as the lifetime of optical annuli. Given the
 194 50 km separation between Skibotn and Ramfjordmoen,
 195 parallax causes vertical extent to appear as horizontal
 196 structure in the image. Plotted in Figure 2 is the magnetic
 197 field line passing through the HF transmitter, with increas-
 198 ing altitude mapping towards the bottom right of the image.
 199 The optical rays appear parallel to the magnetic field line,
 200 strongly suggesting they are not horizontal structures. If the
 201 rays are magnetic field-aligned, they appear to come from
 202 above the HF reflection altitude, projecting upwards from
 203 230 km altitude. This is in contrast to previous observations,
 204 which have shown the optical emission coming from well
 205 below (10s of km) the HF reflection altitude [Haslett and
 206 Megill, 1974; Gustavsson *et al.*, 2001; Kosch *et al.*, 2002b].
 207 It is natural to expect the optical emission to come from
 208 below the source of energetic electrons because the neutral
 209 oxygen density increases with decreasing altitude and
 210 energetic electrons moving upwards will undergo fewer
 211 collisions before escaping into space.

212 [9] The ratio of peak optical intensities for both the
 213 annuli and blobs is $I_{5577}/I_{6300} \approx 1$, which is a clear
 214 indication that the optical excitation mechanism is from a
 215 non-thermal electron population [Gustavsson *et al.*, 2002],
 216 strongly suggesting that plasma turbulence must be accel-
 217 erating a fraction of the electrons. Figure 3 shows the
 218 EISCAT UHF radar backscatter power, from the 12μ s lag
 219 of the tau2 alternating code, covering 5 HF pump cycles
 220 over 20 min. as a superposed epoch, starting at 16:12:00 UT
 221 and including the interval shown in Figure 1. Figure 3
 222 shows a vertical meridional cut through space with the radar

scanning at zenith angles of 3, 6, 9, 12 and 15° south, 223
 spending 4 min. in each position. The radar integration is 5 s, 224
 but this has been post-integrated to 10 s for comparison with 225
 Figure 1. It is clear that backscatter enhancements are 226
 centred on 6 and 15° south for the first 20 s. Thereafter, a 227
 single backscatter enhancement forms at 9° south. After 40 s, 228
 the enhanced backscatter region appears to move between 229
 9° and 12° south. The radar backscatter morphology is 230
 strikingly similar to the optical annulus. Figure 3 shows 231
 the radar backscatter annulus collapsing into a blob within 232
 20 s, whereas the optical annulus in Figure 1 takes 60 s to do 233
 the same. The discrepancy is due to Figure 3 being a 234
 composite of five HF pump cycles and the long radiative 235
 lifetime of O^1D . The radar annulus lifetime was ~ 15 –50 s 236
 throughout this experiment. 237

[10] The radar annulus starts at ~ 235 km, which is near 238
 the HF reflection altitude, as expected for Langmuir turbu- 239
 lence, and then descends to ~ 215 km or lower in some other 240
 cases. This means that the phenomenon starts ~ 20 km, or 241
 ~ 50 kHz, above the 4th gyro-harmonic altitude and appears 242
 to descend approaching the gyro-harmonic at 5.423 MHz. 243
 This is supported by simultaneous stimulated electromag- 244
 netic emission (SEE) measurements (not shown), whose 245
 spectra change distinctly when approaching a gyro-harmonic 246
 frequency [Leyser, 2001, and references therein]. Although 247
 not immediately apparent from Figure 1, detailed analysis 248
 shows that the optical emission appears to descend in the 249
 same way (not shown). The descent in altitude is probably 250
 due to the increase in electron temperature [Gustavsson *et al.*, 251
 2001; Rietveld *et al.*, 2003], which reduces the electron 252
 recombination rate [Robinson, 1989; Gurevich, 1978] there- 253
 by effectively increasing the local plasma density. Since the 254
 HF reflection altitude is a function of electron density, it 255
 must therefore descend. The phenomenon of descending 256
 pump-induced radar backscatter is not new [Djuth *et al.*, 257
 1994] but has not been observed before in the context of 258
 artificially stimulated optical emissions. The steady state 259
 optical blob is different from previous observations where 260
 the optical emission virtually disappeared when pumping on a 261
 gyro-harmonic frequency [Kosch *et al.*, 2002a]. However, 262

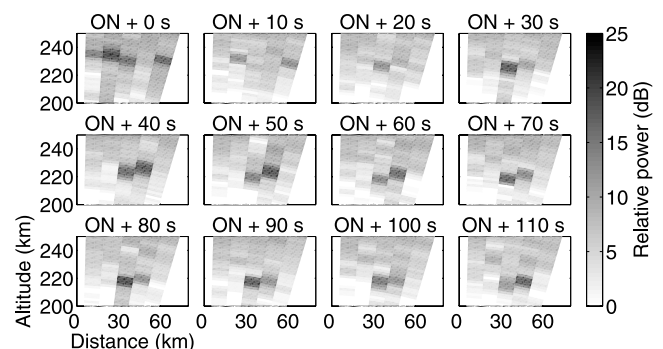


Figure 3. A superposed epoch of EISCAT UHF range-corrected backscatter power starting at 16:12:00 UT, generated from 5 complete HF pump cycles taking 20 min. in total. The radar was scanning at zenith angles of 3, 6, 9, 12 and 15° south. The panel labels indicate the time elapsed after the pump beam was turned on. The integrated radar data resolution is 5.4 km and 10 s. The horizontal axis indicates distance south of EISCAT.

263 Kosch et al. [2002a] performed low-gain magnetic field-
264 aligned HF pumping near the 3rd gyro-harmonic.

265 [11] The 9° south zenith angle region is somehow special
266 at EISCAT and occurs between the Spitze angle (6°S),
267 which is the maximum zenith angle for which the HF pump
268 wave still reaches the highest possible reflection altitude,
269 and the magnetic field-line direction (12.8°S). Isham et al.
270 [1999a, 1999b] devised an HF pulsed pump experiment of
271 low duty cycle (0.2 out of 10 s) away from any gyro-
272 harmonic frequency (4.544 MHz). With the EISCAT UHF
273 radar scanning in 2° steps they observed enhanced ion- and
274 plasma-line UHF backscatter, which maximised between 6
275 and 12.8° south. Their results, and those shown in Figure 3,
276 are clear evidence of Langmuir turbulence, which we
277 believe to be an essential part of the electron accelerating
278 mechanism for the annular artificial optical emissions.

279 3. Conclusions

280 [12] For high-power HF pumping close to the 4th gyro-
281 harmonic, and for the pump beam tilting 9°S only, unstable
282 annular optical structures form, which collapse into blobs
283 whilst descending in altitude. The morphology and time
284 development of the enhanced ion-acoustic radar echoes,
285 which are a proxy for Langmuir turbulence, are similar to
286 the optical signature, at least in the north-south meridian.
287 The pump frequency being close to a gyro-harmonic is
288 consistent with suppression of upper-hybrid turbulence,
289 although no direct observations of this are available. Our
290 experiment provides the first observational evidence that
291 artificial optical emissions may result from Langmuir tur-
292 bulence at high latitudes. The unstable annular structures
293 and the need to tilt the HF beam 9°S remains unexplained.

294 [13] **Acknowledgments.** The authors thank Paul Gallop for analysing
295 the EISCAT radar data and Cesar Otero for plotting the SEE data. EISCAT
296 is owned and operated by a consortium of funding agencies from Finland,
297 France, Germany, Japan, Norway, Sweden and the United Kingdom.

298 References

299 Bernhardt, P. A., W. A. Scales, S. M. Grach et al. (1991), Excitation of
300 artificial airglow by high power radio waves from the "Sura" ionospheric
301 heating facility, *Geophys. Res. Lett.*, *18*, 1477–1480.
302 Djuth, F. T., P. Stubbe, M. P. Sulzer et al. (1994), Altitude characteristics of
303 plasma turbulence excited with the Tromsø superheater, *J. Geophys. Res.*,
304 *99*, 333–339.
305 Gurevich, A. V. (1978), *Nonlinear Phenomena in the Ionosphere*, 370 pp.,
306 Springer-Verlag, New York.
307 Gurevich, A. V., Y. S. Dimant, G. M. Milikh, and V. V. Vas'kov (1985),
308 Multiple acceleration of electrons in the regions of high-power radio-
309 wave reflection in the ionosphere, *J. Atmos. Terr. Phys.*, *47*, 1057–1070.
310 Gustavsson, B., et al. (2001), First tomographic estimate of volume distri-
311 bution of HF-pump enhanced airglow emission, *J. Geophys. Res.*, *106*,
312 29,105–29,123.
313 Gustavsson, B., B. U. E. Brändström, Å. Steen et al. (2002), Nearly
314 simultaneous images of HF-pump enhanced airglow at 6300 Å and
315 5577 Å, *Geophys. Res. Lett.*, *29*(24), 2220, doi:10.1029/2002GL015350.
316 Haslett, J. C., and L. R. Megill (1974), A model of enhanced airglow
317 excited by RF radiation, *Radio Sci.*, *9*, 1005–1019.

Honary, F., T. R. Robinson, D. M. Wright et al. (1999), First direct
318 observations of the reduced striations at pump frequencies close to the
319 electron gyro-harmonics, *Ann. Geophys.*, *17*, 1235–1238. 320
Isham, B., T. Hagfors, E. Mishin et al. (1999a), A search for the location of
321 the HF excitation of enhanced ion acoustic and Langmuir waves with
322 EISCAT and the Tromsø Heater, *Radiophys. Quantum Electr.*, *7*, 607–
323 618. 324
Isham, B., M. T. Rietveld, T. Hagfors et al. (1999b), Aspect angle depen-
325 dence of HF enhanced incoherent backscatter, *Adv. Space Res.*, *24*,
326 1003–1006. 327
Istomin, Y. N., and T. B. Leyser (1997), Small-scale magnetic field-aligned
328 density irregularities excited by a powerful electromagnetic wave, *Phys.*
329 *Plasmas*, *4*, 817–828. 330
Istomin, Y. N., and T. B. Leyser (2003), Electron acceleration by cylindrical
331 upper hybrid oscillations trapped in density irregularities in the iono-
332 sphere, *Phys. Plasmas*, *10*, 2962–2970. 333
Kosch, M. J., T. Hagfors, and E. Nielsen (1998), A new digital all-sky
334 imager experiment for optical auroral studies in conjunction with the
335 Scandinavian twin auroral radar experiment, *Rev. Sci. Instrum.*, *69*,
336 578–584. 337
Kosch, M. J., M. T. Rietveld, T. Hagfors, and T. B. Leyser (2000), High-
338 latitude HF-induced airglow displaced equatorwards of the pump beam,
339 *Geophys. Res. Lett.*, *27*, 2817–2820. 340
Kosch, M. J., M. T. Rietveld, A. J. Kavanagh et al. (2002a), High-latitude
341 pump-induced optical emissions for frequencies close to the third electron
342 gyro-harmonic, *Geophys. Res. Lett.*, *29*(23), 2112, doi:10.1029/
343 2002GL015744. 344
Kosch, M. J., M. T. Rietveld, T. K. Yeoman et al. (2002b), The high-latitude
345 artificial aurora of 21 February 1999: An analysis, *Adv. Pol. Upper*
346 *Atmos. Res.*, *16*, 1–12. 347
Leyser, T. B. (2001), Stimulated electromagnetic emissions by high-
348 frequency electromagnetic pumping of the ionospheric plasma, *Space*
349 *Sci. Rev.*, *98*, 223–328. 350
Mishin, E., H. C. Carlson, and T. Hagfors (2000), On the electron distribu-
351 tion function in the F region and airglow enhancements during HF mod-
352 ification experiments, *Geophys. Res. Lett.*, *27*, 2857–2860. 353
Pedersen, T. R., and H. C. Carlson (2001), First observations of HF heater-
354 produced airglow at the High Frequency Active Auroral Research Pro-
355 gram facility: Thermal excitation and spatial structuring, *Radio Sci.*, *36*,
356 1013–1026. 357
Pedersen, T. R., M. McCarrick, E. Gerken et al. (2003), Magnetic zenith
358 enhancement of HF radio-induced airglow production at HAARP, *Geo-*
359 *phys. Res. Lett.*, *30*(4), 1169, doi:10.1029/2002GL016096. 360
Ponomarenko, P. V., T. B. Leyser, and B. Thidé (1999), New electron
361 gyroharmonic effects in the HF scatter from pump-excited magnetic
362 field-aligned ionospheric irregularities, *J. Geophys. Res.*, *104*,
363 10,081–10,087. 364
Rietveld, M. T., M. J. Kosch, N. F. Blagoveshchenskaya et al. (2003),
365 Ionospheric electron heating, optical emissions, and striations induced
366 by powerful HF radio waves at high latitudes: Aspect angle dependence,
367 *J. Geophys. Res.*, *108*(A4), 1141, doi:10.1029/2002JA009543. 368
Rishbeth, H., and A. P. van Eyken (1993), EISCAT: Early history and the
369 first ten years of operation, *J. Atmos. Terr. Phys.*, *55*, 525–542. 370
Robinson, P. A. (1997), Nonlinear wave collapse and strong turbulence,
371 *Rev. Mod. Phys.*, *69*, 507–573. 372
Robinson, T. R. (1989), The heating of the high latitude ionosphere by high
373 power radio waves, *Phys. Rep.*, *179*, 79–209. 374
Stubbe, P. (1996), Review of ionospheric modification experiments at
375 Tromsø, *J. Atmos. Terr. Phys.*, *58*, 349–368. 376

F. Honary, M. J. Kosch, and A. Senior, Communication Systems, 378
Lancaster University, Lancaster LA1 4YR, UK. (m.kosch@lancaster.ac.uk) 379

B. Isham, EISCAT Scientific Association, N-9171 Longyearbyen, 380
Norway. 381

A. J. Kavanagh, High Altitude Observatory, National Center for 382
Atmospheric Research, Boulder, CO 80307-3000, USA. 383

I. W. McCrea, Rutherford-Appleton Laboratory, Didcot OX11 0QX, UK. 384

M. T. Rietveld, EISCAT Scientific Association, N-9027 Ramfjordbotn, 385
Norway. 386